PHYSICAL REVIEW MATERIALS **3**, 125801 (2019)

Ti interstitial flows giving rutile TiO_2 reoxidation process enhancement in (001) surface

Tom Ichibha[*]
School of Information Science, JAIST, 1-1 Asahidai, Nomi, Ishikawa 923-1292, Japan
and Materials Science and Technology Division, Oak Ridge National Laboratory, Oak Ridge, Tennessee 37831, USA

Anouar Benali[†]
Computational Science Division, Argonne National Laboratory, 9700 Cass Avenue, Lemont, Illinois 60439, USA

Kenta Hongo
Research Center for Advanced Computing Infrastructure, JAIST, 1-1 Asahidai, Nomi, Ishikawa 923-1292, Japan;
Center for Materials Research by Information Integration, Research and Services Division of Materials Data and Integrated System,
National Institute for Materials Science, 1-2-1 Sengen, Tsukuba 305-0047, Japan;
PRESTO, Japan Science and Technology Agency, 4-1-8 Honcho, Kawaguchi-shi, Saitama 322-0012, Japan;
and Computational Engineering Applications Unit, RIKEN, 2-1 Hirosawa, Wako, Saitama 351-0198, Japan

Ryo Maezono
School of Information Science, JAIST, 1-1 Asahidai, Nomi, Ishikawa 923-1292, Japan
and Computational Engineering Applications Unit, RIKEN, 2-1 Hirosawa, Wako, Saitama 351-0198, Japan

(Received 9 September 2019; published 2 December 2019)

We revisited *ab initio* evaluations of the barrier energies along the possible diffusion paths of the defects in rutile TiO_2 by using a diffusion Monte Carlo method. We found that Ti interstitials hopping along the c axis are identified as the major diffusion directing to the (001) surface, contradicting any of the previous density functional theory studies. Our finding reasonably explains recent experiments reporting that the photocatalytic activity in the (001) surface is superior to that in the (110) surface: The faster Ti diffusion directing to the (001) surface leads to the better self-compensation ability and maintains its photocatalytic activity.

DOI: 10.1103/PhysRevMaterials.3.125801

I. INTRODUCTION

TiO_2 is a representative transition metal oxide with various applications such as white paints, photovoltaic cells, and rechargeable batteries [1–5]. Its photocatalysis ability is especially useful for water splitting and antipollution/bacteria coating [6]. During the photocatalysis reaction, O ions are easily detached from the surface [7], and hence one may anticipate the depression of the photocatalysis ability. Yet in reality, the surface gets O ions from the atmosphere, and the photocatalysis ability is maintained [7].

One of the most useful properties is the reoxidization of rutile surface state even in a vacuum keeping its stoichiometry. The property is promising for such applications in space as a coating over the solar panels of spaceships keeping its performance of photoreactions [8]. The reoxidization in a vacuum is explained to be caused by the possible ionic flows of Ti interstitials (Ti_i) and/or oxygen vacancies (V_O) from within the bulk toward the surface compensating the stoichiometry kept unchanged [7]. However, a consensus on the diffusion process of point defects has yet to be established and controversy remains even for within a simple bulk structure [9,10].

Surveying the controversy, the points to be clarified here would be summarized into two simple questions: (a) which defect (Ti_i or V_O) is the dominant, and (b) which diffusion path is dominating. An experiment of the reoxidization of the sputtered rutile $TiO_2(110)$ surface annealed in ultrahigh vacuum [11] reports a conclusion that Ti_i plays a major role in the process. This is also supported from *ab initio* studies using density functional theory (DFT) [9,10], predicting lower energy barriers for Ti_i than V_O diffused in any direction. Taking Ti_i being superior to V_O, the controversy exists on which path gives faster diffusion, parallel ($c_\parallel$) or perpendicular ($c_\perp$) to the c direction (parallel to the Ti chain in the crystal). While two old experiments [12,13] report contradicting conclusions to each other, both of the previous DFT works [9,10] support $c_\perp$ as the major diffusion process.

One of the major origins of the energy barrier required for a defect to move beyond is the interaction between the surrounding atoms. It is therefore sensitive to how the electronic distribution of a defect spreads to contact with the neighboring atoms. Here we remind one that such a spreading is poorly estimated by the conventional type of DFT using local-density approximation (LDA) or generalized gradient approximation (GGA) type exchange-correlation (XC) functionals. In these XCs, the cancellation of the self-interaction is incomplete, leading to a spurious delocalization of the charge distribution [14,15]. The shortcoming is known to be recovered to some

---

[*] ichibha@icloud.com

[†] benali@anl.gov

2475-9953/2019/3(12)/125801(5)

extent by using DFT + U methods [16,17] mainly curing the self-interaction problem but also the description of electronic correlations [16,17]. The method is reported [17] to achieve fairly good descriptions of the ground states in the systems with transition metal elements, which have been regarded as a representative challenge for the electronic correlations. The drawback for the method has been how to choose the adjustable parameters, U and J, by which the method is known to be sensitive in its predictions [17,18]. There have been some advances on this matter by such approaches to determine U by some variational scheme [19]. In the scheme, however, J is practically fixed at zero while the choice of J can seriously affect the prediction [18]. The remedy by DFT + U would, therefore, be limited to some extent toward a perfect description of the problem.

We hence revisit the evaluation of the energy barriers for defects diffusion by applying the diffusion Monte Carlo method (DMC) [20]. The method is based on the variational principles in which the delicate balance between the exchange and correlation [21] can be handled satisfactorily without requiring any arbitrary modeling. The method has successfully been applied to the present $\mathrm{TiO_2}$ system in previous works [4,5,22,23]. We confirmed that $\mathrm{Ti_i}$ is the dominant defect to diffuse, contributing to the reoxidation process with an energy barrier lower than that for V_O, being consistent with previous DFT works [9,10]. A striking finding we made is that the previous DFT prediction supporting $c_\perp$ is reverted into $c_\parallel$ when the cancellation of the self-interaction is considered by using "+U" or DMC. The results support a better reoxidation activity on the (001) surface, consistent with experiments [24,25] reporting that said surface has almost the highest photocatalytic activity.

II. SYSTEM

The rutile structure of $\mathrm{TiO_2}$ is shown in Fig. 1. It consists of Ti chains along the c axis. Ti positions along the axis are shifted by a 1/2 period between the neighboring chains. $\mathrm{Ti_i}$ is formed in the middle of the Ti chains as shown in Fig. 1 [9], for which two possible diffusion paths ($c_\parallel$ and $c_\perp$) are of interest [9]. The hopping along $c_\perp$ is described as the "kick-out mechanism" [26]. For V_O, three paths, I–III in Fig. 1, are considered [9]. We evaluated barrier energies along these five paths for fully positively charged defects ($\mathrm{Ti_i^{\bullet\bullet\bullet\bullet}}$, $V_\mathrm{O}^{\bullet\bullet}$), as summarized in Table I. Previous theoretical works [9,27] predict only the possibility of getting $\mathrm{Ti_i^{\times}}$, $\mathrm{Ti_i^{\bullet\bullet\bullet\bullet}}$, $V_\mathrm{O}^{\times}$, $V_\mathrm{O}^{\bullet\bullet}$ depending on the Fermi level, where, for example, $\mathrm{Ti_i^{\bullet\bullet\bullet\bullet}}$ represents +4 charges per Ti interstitial (less by four electrons per defect than the neutral state) and $V_\mathrm{O}^{\times}$ represents ±0 charges per O vacancy. Experimentally, the charged defects are confirmed to be realized in the surface [28], and hence we took $\mathrm{Ti_i^{\bullet\bullet\bullet\bullet}}$ and $V_\mathrm{O}^{\bullet\bullet}$ as the defects to be investigated. The results for the neutral defect, $\mathrm{Ti_i^{\times}}$, are also shown in Table I, which are referred to only in further discussions. The descriptions henceforth are therefore about the $\mathrm{Ti_i^{\bullet\bullet\bullet\bullet}}$ and $V_\mathrm{O}^{\bullet\bullet}$ unless noted otherwise.

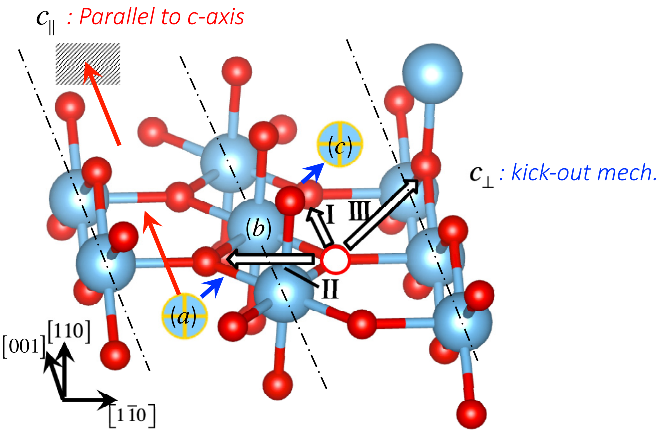

FIG. 1. Five possible paths for defect diffusions of $\mathrm{Ti_i}$ (blue and red arrows) and V_O (white arrows) in bulk rutile $\mathrm{TiO_2}$. The large blue balls are Ti ions and the small red balls are oxygen ions. Ti atoms are located along the c axis ([001] direction). In $c_\perp$ diffusion (blue arrow), a $\mathrm{Ti_i}$ kicks a Ti on the axis out to make another $\mathrm{Ti_i}$ in the opposite side (kick-out diffusion [26]), directing along the [100] or [010] axis. The diffusion along the path $c_\parallel$ (red arrow) directs toward the [001] surface as shown by a hatched square.

TABLE I. Barrier energies of $\mathrm{Ti_i}$ ($c_\parallel$ and $c_\perp$) and V_O (I, II, and III) paths evaluated by various methods, including previous works [9,10]. All the predictions are made for fully positively charged defects ($\mathrm{Ti_i^{\bullet\bullet\bullet\bullet}}$, $V_\mathrm{O}^{\bullet\bullet}$), except "DMC ($\mathrm{Ti_i^{\times}}$)" (neutral), which is shown for a reference in discussions. The geometries to evaluate the barrier are optimized each to neutral and charged states, independently.

	$\mathrm{Ti_i}$		V_O		
	$c_\parallel$	$c_\perp$	I	II	III
GGA-PW91 [9]	0.37	**0.225**	1.77	$\underline{0.69}$	1.1
GGA-PW91 [10]	0.31	**0.23**			
LDA+U	**0.54**	0.90	2.42	1.60	$\underline{1.36}$
DMC	**0.4(1)**	0.9(1)	2.0(1)	$\underline{0.9(2)}$	1.7(1)
DMC ($\mathrm{Ti_i^{\times}}$)	2.6(4)	1.6(1)			

III. CALCULATION DETAILS

We made a simulation cell by putting a point defect in a 2 × 2 × 3 supercell of the ideal rutile $\mathrm{TiO_2}$ unit cell. We optimized the crystal structures at the *edge* and the *saddle* points of the states along the diffusion paths using the PAW-DFT method implemented on VASP [29]. The optimizations are made to relax internal atomic positions within a cell under the fixed lattice constants at experimental values [30]. The energy cutoff is 700 eV and the spacing of the k-mesh sampling is denser than 0.50 $\mathrm{\AA^{-1}}$. Atomic positions are relaxed until the forces on any ions are suppressed less than 0.01 eV/Å. The structures at the saddle states are determined by the climbing nudged elastic band (c-NEB) method [31]. A diffusion path is expressed with 5 or 15 intermediate states between the edge states. Since one of the states must be converged to be the saddle state in c-NEB [31], the number of states does not affect the barrier energy prediction but affects the convergence of the relaxation.

We applied DMC to evaluate the energies at the edge and saddle structures using QMCPACK [32]. We used Slater-Jastrow type trial wave functions [20,33]. Orbital functions used in the Slater determinant are generated by the LDA + U method implemented in QUANTUM ESPRESSO [34]. We used a Hubbard correction value of U = 4.86 eV from a previous work [22], giving the best accessible nodal surface within this formalism, guaranteeing the lowest energy for TiO_2 from the variational principle. Core electrons in both Ti and O atoms were described by the use of a hard norm-conserving pseudopotential developed to reproduce accurately all electron results with the context of many-body theory and as described in previous works [22]. The orbitals are generated with a 300 Ry energy cutoff and the thermodynamic limit is reached with a $2 \times 2 \times 2$ k-mesh size. The Jastrow factor consists of one-, two-, and three-body terms amounting to 144 variational parameters in total, which are optimized by variational Monte Carlo calculations [20,33]. The parameters are optimized by the scheme to minimize a hybridization of energy and variance in 7:3. Twist averaging over the boundary conditions is taken into account with a $2 \times 2 \times 2$ grid [35]. We estimated a time-step bias by a linear extrapolation of the energies obtained at two time steps, $dt = 0.020$ and 0.005 a.u.$^{-1}$. It is confirmed that the time-step bias is proportional to dt in a range of $dt < 0.020$ a.u.$^{-1}$. We set a target population of walkers to be 4000. Practically, this size target population is large enough to suppress a population control error.

IV. RESULTS AND DISCUSSION

Table I summarizes the results of the barrier energies along each path. Looking at the lowest barrier energies (shown in bold), all methods, consistent with each other, predict Ti_i as the preferred diffusion carrier. A striking difference is found between our current result and the previous ones regarding the Ti_i preferred diffusion path. Updated predictions by LDA + U and DMC support $c_\parallel$ as the dominant flow, directing towards the (001) surface while $c_\perp$ directing towards the (100) or (010) surface. The prediction here may explain the experimental observation of the photocatalytic activity being enhanced at the (001) surface compared to the (100) surface [24,25]. We note that LDA + U and DMC give different predictions about the fastest diffusion path for V_O. Our final DMC prediction gives path II as the fastest path for oxygen vacancy diffusion (V_O). However, path II alone cannot produce any diffusion flows because sites in this path are disconnected from each other. For V_O's to diffuse globally in the bulk a combination of path I/III with path II is needed, otherwise V_O's will be constrained to the isolated sites in path II.

When compared to our DMC results, previous GGA-DFT calculations show a significant underestimation of barrier energies. Even using "the same fixed geometry relaxed with DFT + U" in GGA and DFT + U calculations, the trend of underestimation is confirmed. This can be attributed to the fact that GGA generally underestimates a cohesive energy [36], since a defect is more weakly combined with the surrounding ions than reality, making its hopping easier.

As can be seen in Table I, evaluating the diffusion path of the neutral defect DMC ($Ti_i^\times$), the most favorable diffusion path is $c_\perp$, opposite to what is found for a charged defect. This might be a clue to understanding why the present result contradicts the previous DFT works, as well as to understanding the contradiction in the earlier experiments [12,13]: One of the dominant factors to determine the preferred diffusion path could be the ionic radius of the defects, which is reduced when they are positively charged to reduce accompanying electrons. The sensitive dependence on the choice of XC potentials in Table I could support this, because the estimation of the radius is known to be sensitive to how the self-interaction is carefully treated [15]. Poor treatments are expected to give a spurious delocalization of distribution leading to a larger radius [14]. The Hubbard "+U" correction is introduced to cancel out this, and hence corrects the radius to be smaller. Previous GGAs are therefore suspected to give overestimations of the radius, namely, *spuriously less positively charged defects* [14]. Our Bader analyses using a scheme described in Ref. [37] actually showed that the Perdew-Burke-Ernzerhof (PBE) functional has a larger volume than LDA + U, predicting 6.765 and 6.914 Å^3 for LDA + U and PBE, respectively.

An earlier experiment [13] supporting $c_\perp$ as the preferred path was performed at high temperatures ranging from 1000 to 1500 K. It is shown through simulation that the electronic distribution in the valence region is expanded with high temperatures [38]. The high-temperature experiment suggests a less positively charged defect favoring the $c_\perp$ path. This behavior is confirmed by our DMC ($Ti_i^\times$) calculation on a neutral defect (see Table I), which has a larger Bader volume (7.690 Å^3) than $Ti_i^{\bullet\bullet\bullet\bullet}$ (6.765 Å^3).

The faster ionic flow, Ti_i, in the [001] direction as in our updated prediction would explain the experimental facts fairly reasonably as follows: In the photochemical reactions without any oxygen compensations such as those with Ag^+ ions in an aqueous solution, the enhanced reactivities are actually observed when using the (001) surface [24,25,39]. Aiming to recover desorbed oxygens by catalytic reduction processes, Ti ions are required to flow from a surface into the bulk inside so that the stoichiometry at the surface can be kept to support the reactions. Having the surface perpendicular to the faster axis would enhance such ionic flows, and then the reactions are accelerated. We also note that there are contradicting reports that the (001) surface gives less reactivity in some systems [39,40]. When the roughness gets reduced to the atomic scale (~1 nm), the (001) surface becomes less reactive than other surface directions. In this case, however, the reactivity also gets suppressed by a couple of orders [39,40]. Under such a reduced reactivity, the desorptions of oxygen atoms become reluctant, and hence the self-compensation process would become a secondary factor not dominating the reaction anymore, being not contradictory to our prediction.

V. CONCLUSION

In conclusion, we performed *ab initio* evaluations of the energy barriers for defects of Ti interstitials and oxygen vacancies using LDA + U and DMC methods. Ti interstitials diffusing along the Ti chains (c axis) are predicted to give the lowest energy barrier, being the most likely origin of the atomic flow toward the [001] surface supporting the surface reoxidizations. The result is consistent with the photocatalytic activity in the (001) surface being superior to (100) as experimentally observed [24,25]. The prediction is found to be sensitive to how carefully the cancellation of self-interactions is taken into account, not reproduced by the conventional DFT with nonhybrid XC functionals [9,10]. The cancellation critically changes the radius of the defects interacting with surrounding atoms, which was overestimated by the previous DFT works [9,10].

ACKNOWLEDGMENTS

An award of computer time was provided by the Innovative and Novel Computational Impact on Theory and Experiment (INCITE) program. This research used resources of the Argonne Leadership Computing Facility, which is a DOE Office of Science User Facility supported under Contract No. DE-AC02-06CH11357, and the Research Center for Advanced Computing Infrastructure (RCACI) at JAIST. T.I. is grateful for financial suport from Grant-in-Aid for JSPS Research Fellow (Grant No. 18J12653). A.B. is supported by the US Department of Energy, Office of Science, Basic Energy Sciences, Materials Sciences and Engineering Division, as part of the Computational Materials Sciences Program and Center for Predictive Simulation of Functional Materials. K.H. is grateful for financial support from a KAKENHI grant (Grant No. JP17K17762), a Grant-in-Aid for Scientific Research on Innovative Areas "Mixed Anion" project (Grant No. JP16H06439) from MEXT, PRESTO (Grant No. JPMJPR16NA), and the Materials Research by Information Integration Initiative (MI^{2}I) project of the Support Program for Starting Up Innovation Hub from Japan Science and Technology Agency (JST). R.M. is grateful for financial support from MEXT-KAKENHI (Grants No. 19H04692 and No. 16KK0097), from Toyota Motor Corporation, from I-O DATA Foundation, from the Air Force Office of Scientific Research (AFOSR-AOARD/FA2386-17-1-4049;FA2386-19-1-4015), and from JSPS Bilateral Joint Projects (with India DST). R.M. and K.H. are also grateful for financial support from MEXT-FLAGSHIP2020 (Grants No. hp190169 and No. hp190167).

---

[1] M. Sajedi Alvar, M. Javadi, Y. Abdi, and E. Arzi, Enhancing the electron lifetime and diffusion coefficient in dye-sensitized solar cells by patterning the layer of TiO_2 nanoparticles, J. Appl. Phys. **119**, 114302 (2016).

[2] G. Longoni, R. L. Pena Cabrera, S. Polizzi, M. D'Arienzo, C. M. Mari, Y. Cui, and R. Ruffo, Shape-controlled TiO_2 nanocrystals for Na-ion battery electrodes: The role of different exposed crystal facets on the electrochemical properties, Nano Lett. **17**, 992 (2017).

[3] M. Abbasnejad, M. R. Mohammadizadeh, and R. Maezono, Structural, electronic, and dynamical properties of Pca21-TiO_2 by first principles, Europhys. Lett. **97**, 56003 (2012).

[4] M. Abbasnejad, E. Shojaee, M. R. Mohammadizadeh, M. Alaei, and R. Maezono, Quantum Monte Carlo study of high-pressure cubic TiO_2, Appl. Phys. Lett. **100**, 261902 (2012).

[5] S. K. Gharaei, M. Abbasnejad, and R. Maezono, Bandgap reduction of photocatalytic TiO_2 nanotube by Cu doping, Sci. Rep. **8**, 14192 (2018).

[6] T. Verdier, M. Coutand, A. Bertron, and C. Roques, Antibacterial activity of TiO_2 photocatalyst alone or in coatings on *E. coli*: The influence of methodological aspects, Coatings **4**, 670 (2014).

[7] K. T. Park, M. Pan, V. Meunier, and E. W. Plummer, Reoxidation of $TiO_2(110)$ via Ti interstitials and line defects, Phys. Rev. B **75**, 245415 (2007).

[8] F. Urayama, M. Furukawa, K. Ozawa, M. Tosa, and H. Kimura, Study on molecular contamination prevention by using photocatalysts under vacuum conditions, Aerospace Technol. Jpn. **6**, 81 (2007).

[9] H. Iddir, S. Öğüt, P. Zapol, and N. D. Browning, Diffusion mechanisms of native point defects in rutile TiO_2: *Ab initio* total-energy calculations, Phys. Rev. B **75**, 073203 (2007).

[10] A. M. Asaduzzaman and P. Krüger, A first principles study on charge dependent diffusion of point defects in rutile TiO_2, J. Phys. Chem. C **114**, 19649 (2010).

[11] M. A. Henderson, A surface perspective on self-diffusion in rutile TiO_2, Surf. Sci. **419**, 174 (1999).

[12] H. B. Huntington and G. A. Sullivan, Interstitial Diffusion Mechanism in Rutile, Phys. Rev. Lett. **14**, 177 (1965).

[13] K. Hoshino, N. Peterson, and C. Wiley, Diffusion and point defects in TiO_{2-x}, J. Phys. Chem. Solids **46**, 1397 (1985).

[14] P. Gori-Giorgi, J. G. Ágyán, and A. Savin, Charge density reconstitution from approximate exchange-correlation holes, Can. J. Chem. **87**, 1444 (2009).

[15] J. L. Bao, L. Gagliardi, and D. G. Truhlar, Self-interaction error in density functional theory: An appraisal, J. Phys. Chem. Lett. **9**, 2353 (2018).

[16] N. J. Mosey and E. A. Carter, *Ab initio* evaluation of Coulomb and exchange parameters for DFT + U calculations, Phys. Rev. B **76**, 155123 (2007).

[17] B. Himmetoglu, A. Floris, S. de Gironcoli, and M. Cococcioni, Hubbard-corrected DFT energy functionals: The LDA+U description of correlated systems, Int. J. Quant. Chem. **114**, 14 (2014).

[18] S. A. Tolba, K. M. Gameel, B. A. Ali, H. A. Almossalami, and N. K. Allam, The DFT+U: Approaches, accuracy, and applications, in *Density Functional Calculations*, edited by G. Yang (IntechOpen, Rijeka, 2018), Chap. 1.

[19] M. Cococcioni and S. de Gironcoli, Linear response approach to the calculation of the effective interaction parameters in the LDA + U method, Phys. Rev. B **71**, 035105 (2005).

[20] W. M. C. Foulkes, L. Mitas, R. J. Needs, and G. Rajagopal, Quantum Monte Carlo simulations of solids, Rev. Mod. Phys. **73**, 33 (2001).

[21] Y. Takada and H. Yasuhara, Momentum distribution function of the electron gas at metallic densities, Phys. Rev. B **44**, 7879 (1991).

[22] Y. Luo, A. Benali, L. Shulenburger, J. T. Krogel, O. Heinonen, and P. R. C. Kent, Phase stability of TiO_2 polymorphs from diffusion quantum Monte Carlo, New J. Phys. **18**, 113049 (2016).

[23] J. Trail, B. Monserrat, P. López Ríos, R. Maezono, and R. J. Needs, Quantum Monte Carlo study of the energetics of the rutile, anatase, brookite, and columbite TiO_2 polymorphs, Phys. Rev. B **95**, 121108(R) (2017).

[24] J. B. Lowekamp, G. S. Rohrer, P. A. M. Hotsenpiller, J. D. Bolt, and W. E. Farneth, Anisotropic photochemical reactivity of bulk TiO_2 crystals, J. Phys. Chem. B **102**, 7323 (1998).

[25] P. A. Morris Hotsenpiller, J. D. Bolt, W. E. Farneth, J. B. Lowekamp, and G. S. Rohrer, Orientation dependence of photochemical reactions on TiO_2 surfaces, J. Phys. Chem. B **102**, 3216 (1998).

[26] J. Sasaki, N. Peterson, and K. Hoshino, Tracer impurity diffusion in single-crystal rutile (TiO_{2-x}), J. Phys. Chem. Solids **46**, 1267 (1985).

[27] H.-Y. Lee, S. J. Clark, and J. Robertson, Calculation of point defects in rutile TiO_2 by the screened-exchange hybrid functional, Phys. Rev. B **86**, 075209 (2012).

[28] J. Nowotny, M. A. Alim, T. Bak, M. A. Idris, M. Ionescu, K. Prince, M. Z. Sahdan, K. Sopian, M. A. Mat Teridi, and W. Sigmund, Defect chemistry and defect engineering of TiO_2-based semiconductors for solar energy conversion, Chem. Soc. Rev. **44**, 8424 (2015).

[29] G. Kresse and J. Furthmüller, Efficient iterative schemes for *ab initio* total-energy calculations using a plane-wave basis set, Phys. Rev. B **54**, 11169 (1996).

[30] D. G. Isaak, J. D. Carnes, O. L. Anderson, H. Cynn, and E. Hake, Elasticity of TiO_2 rutile to 1800 K, Phys. Chem. Minerals **26**, 31 (1998).

[31] G. Henkelman and H. Jónsson, Improved tangent estimate in the nudged elastic band method for finding minimum energy paths and saddle points, J. Chem. Phys. **113**, 9978 (2000).

[32] J. Kim, A. D. Baczewski, T. D. Beaudet, A. Benali, M. C. Bennett, M. A. Berrill, N. S. Blunt, E. J. L. Borda, M. Casula, D. M. Ceperley, S. Chiesa, B. K. Clark, R. C. Clay, K. T. Delaney, M. Dewing, K. P. Esler, H. Hao, O. Heinonen, P. R. C. Kent, J. T. Krogel *et al.*, QMCPACK: An open source *ab initio* quantum Monte Carlo package for the electronic structure of atoms, molecules and solids, J. Phys.: Condens. Matter **30**, 195901 (2018).

[33] R. Maezono, Optimization of many-body wave function, J. Comput. Theor. Nanosci. **6**, 2474 (2009).

[34] P. Giannozzi, S. Baroni, N. Bonini, M. Calandra, R. Car, C. Cavazzoni, D. Ceresoli, G. L. Chiarotti, M. Cococcioni, I. Dabo, A. D. Corso, S. de Gironcoli, S. Fabris, G. Fratesi, R. Gebauer, U. Gerstmann, C. Gougoussis, A. Kokalj, M. Lazzeri, L. Martin-Samos *et al.*, QUANTUM ESPRESSO: A modular and open-source software project for quantum simulations of materials, J. Phys.: Condens. Matter **21**, 395502 (2009).

[35] C. Lin, F. H. Zong, and D. M. Ceperley, Twist-averaged boundary conditions in continuum quantum Monte Carlo algorithms, Phys. Rev. E **64**, 016702 (2001).

[36] M. Arrigoni and G. K. Madsen, Comparing the performance of LDA and GGA functionals in predicting the lattice thermal conductivity of III-V semiconductor materials in the zincblende structure: The cases of AlAs and BAs, Comput. Mater. Sci. **156**, 354 (2019).

[37] W. Tang, E. Sanville, and G. Henkelman, A grid-based Bader analysis algorithm without lattice bias, J. Phys.: Condens. Matter **21**, 084204 (2009).

[38] V. Shah, B. Sanghavi, R. Ramchandani, M. P. Gururajan, and T. R. S. Prasanna, Finite temperature electronic structure of diamond and silicon, arXiv:1802.07179.

[39] A. Fujishima, X. Zhang, and D. A. Tryk, TiO_2 photocatalysis and related surface phenomena, Surf. Sci. Rep. **63**, 515 (2008).

[40] Y. Yamamoto, K. Nakajima, T. Ohsawa, Y. Matsumoto, and H. Koinuma, Preparation of atomically smooth TiO_2 single crystal surfaces and their photochemical property, Jpn. J. Appl. Phys. **44**, L511 (2005).